Surface Structure and Interface Dynamics of Alkanethiol Self-Assembled Monolayers on Au(111)

Jaegeun Noh,*,† Hiroyuki S. Kato,‡ Maki Kawai,‡ and Masahiko Hara§,⊥

Advanced Nanomaterials Laboratory, Department of Chemistry, Hanyang University, 17 Haengdang-dong, Seoungdong-gu, Seoul 133-791, Korea, Surface Chemistry Laboratory, RIKEN, 2-1 Hirosawa, Wako, Saitama 351-0198, Japan, Department of Electronic Chemistry, Tokyo Institute of Technology, 4259 Nagatsuta, Midoriku, Yokohama 226-8502, Japan, and Local Spatio-Temporal Functions Laboratory, Frontier Research System, RIKEN, 2-1 Hirosawa, Wako, Saitama 351-0198, Japan

Received: September 29, 2005; In Final Form: November 17, 2005

Scanning tunneling microscopy (STM) and high-resolution electron energy loss spectroscopy (HREELS) were used to examine the structural transitions and interface dynamics of octanethiol (OT) self-assembled monolayers (SAMs) caused by long-term storage or annealing at an elevated temperature. We found that the structural transitions of OT SAMs from the c(4 × 2) superlattice to the (6 × $\sqrt{3}$) superlattice resulting from long-term storage were caused by both the dynamic movement of the adsorbed sulfur atoms on several adsorption sites of the Au(111) surface and the change of molecular orientation in the ordered layer. Moreover, it was found that the chemical structure of the sulfur headgroups does not change from monomer to dimer by the temporal change of SAMs at room temperature. Contrary to the results of the long-term-stored SAMs, it was found that the annealing process did not modify either the interfacial or chemical structures of the sulfur headgroups or the two-dimensional c(4 × 2) domain structure. Our results will be very useful for a better understanding of the interface dynamics and stability of sulfur atoms in alkanethiol SAMs on Au(111) surfaces.

Introduction

Alkanethiol self-assembled monolayers (SAMs) on gold surfaces have drawn considerable attention in recent years, as they are an ideal model system for understanding the interfacial phenomena of organic molecules and have many potential technological applications such as wetting, molecular recognition, nanopatterning, and molecular electronics.[1−8] Several fundamental features of SAMs such as molecular structures, growth processes, stability, and interface properties have been thoroughly characterized and elucidated by research groups using surface sensitive spectroscopy and microscopy.[9−14] It is known that alkanethiols at saturation coverage form a hexagonal ($\sqrt{3} \times \sqrt{3}$)R30° structure, where the sulfur atoms are assumed to be adsorbed on the hollow site of the Au(111) lattice.[15−18] In addition, high-resolution scanning tunneling microscopy (STM) measurements revealed that the stable structure of alkanethiol SAMs is a c(4 × 2) or (3 × 2$\sqrt{3}$) superlattice with several different height protrusions in the unit cell.[19−24] The different molecular features in STM images may be due to the height difference of the terminal methyl groups caused by a twisting of the chain axis of adsorbed molecules or by the different adsorption sites of the sulfur headgroups. A multiple-adsorption-site model, which originates from the dimerization of the sulfur headgroups for alkanethiol SAMs on Au(111), has been suggested from the results of several experimental techniques including grazing angle X-ray diffraction,[25] sum frequency generation,[26] X-ray standing wave,[27] and thermal desorption spectroscopy.[27] The STM imaging mechanism for SAMs is presently unclear and under discussion.

Contrary to an early theoretical study suggesting that the hollow site is the most favorable,[18] recent studies have reported that the most stable site is the bridge site.[28−30] However, these results may not be generally applicable for various alkanethiol SAMs with different chain lengths because such theoretical approaches have mainly been performed on the simplest alkanethiol SAMs containing only one methyl group. Our recent high-resolution electron energy loss spectroscopy (HREELS) measurements revealed that the adsorption sites in alkanethiol SAMs are complicated and depend on the alkyl chain lengths.[12] In addition, our molecularly resolved STM study for octanethiol SAMs elucidated structural dynamics with phase transitions from the c(4 × 2) superlattice to the (6 × $\sqrt{3}$) superlattice after long-term storage. This phase transition is not due to a change in surface coverage during the measured time periods because the (6 × $\sqrt{3}$) superlattice has the same surface density as the c(4 × 2) superlattice.[32] The reason for such structural transitions is still unclear. Therefore, for further applications of SAM-based devices, it is necessary to understand the interface dynamics and stability of the sulfur headgroups adsorbed on Au(111) in long-term storage. In this paper, we will provide clear answers for the following questions that have not previously been addressed: (1) Is the conversion of adsorption sites dependent on the time evolution of SAMs, and (2) can the dimerization of sulfur headgroups proceed after long-term storage at room temperature? In addition, to compare the structural and interfacial dynamics of long-term-stored SAMs, we examined the annealed octanethiol (OT) SAMs at an elevated temperature. As we demonstrated in the previous paper,[12] HREELS measurements can reveal the bonding features of sulfur headgroups at

* Corresponding author. Phone: +82-2-2220-0938. Fax: +82-2-2299-0762. E-mail: jgnoh@hanyang.ac.kr.
† Hanyang University.
‡ Surface Chemistry Laboratory, RIKEN.
§ Tokyo Institute of Technology.
⊥ Local Spatio-Temporal Functions Laboratory, Frontier Research System, RIKEN.

10.1021/jp055538b CCC: $33.50
Published on Web 01/07/2006

low-frequency regions, and high-resolution STM images can provide real features at the molecular level.

Experimental Section

The Au(111) substrates on mica were prepared by vacuum deposition as reported in the previous paper.[33] Octanethiol (OT, n-$CH_3(CH_2)_7SH$) SAMs were prepared by dipping the Au(111) substrates into a freshly prepared 1 mM ethanol solution for 1 day. After the SAM samples were removed from the solutions, they were rinsed thoroughly with pure ethanol to remove physisorbed molecules from the surface.

To examine time-dependent two-dimensional structures, molecular orientations, and adsorption states of the sulfur headgroups on Au(111), the OT SAMs were immediately put into a Petri dish and completely sealed with a vinyl bag under a vacuum at ~400 Torr using an automatic vacuum-seal machine to prevent air oxidation and contamination of the monolayer at room temperature for 3 and 6 months. The SAM samples were then kept under dark conditions for a given storage period. In addition, the annealed OT SAMs were prepared under a N_2 atmosphere of 1 atm for 30 min at 50 and 100 °C to investigate the packing structure of SAMs and the changes in the chemical structure of sulfur headgroups by annealing. The SAM samples were then rinsed with ethanol prior to the STM and HREELS measurements.

STM measurements were performed with a NanoScope E instrument (Veeco, Santa Barbara, CA) and a commercially available Pt/Ir tip (80:20). All STM images were obtained under ambient conditions in the constant current mode using tunneling currents between 150 and 600 pA and a sample bias between 350 and 800 mV (sample positive).

HREELS measurements were performed in an ultrahigh-vacuum (UHV) system ($<2 \times 10^{-8}$ Pa) equipped with a sample entry system and a set of a monochromator and an electron energy analyzer (Specs GmbH: DELTA 0.5) for HREELS.[34] All spectra were measured at room temperature using a primary beam energy of 3.5 eV and an incidence angle of 60° from the surface normal. For the specular spectra, an intense elastic peak was obtained with a full width at half-maximum of <35 cm^{-1}. The typical elastic-peak current was 0.05 pA for fresh samples. The frequency accuracy for all spectra contained in the present report was approximately ± 10 cm^{-1} ($=1.2$ meV).

In the specular spectra of HREELS, the signals contain both dipole- and impact-scattering components.[35] The selection rule for dipole scattering is the same as that for infrared reflection absorption spectroscopy (IRAS)[36] and is useful for characterizing the adsorption structures. To isolate the dipole-scattering components, off-specular spectra consisting of impact-scattering components were measured at a detection angle of 42° and were plotted with the specular spectra after an intensity correction for the detection angle difference assuming an isotropic distribution, that is, a factor of cos 60°/cos 42°. We confirmed that all of the results presented in this paper were reproducible between different prepared samples.

Results and Discussion

The STM images in Figure 1 show the dynamic structural transitions of OT SAMs from the c(4 × 2) superlattice to the (6 × √3) superlattice due to long-term storage. The c(4 × 2) superlattice was observed from the as-deposited OT SAM samples formed after 1 day of immersion of the Au(111) substrate in 1 mM ethanol solution, as observed in previous studies of OT SAMs (Figure 1a).[19,22] After 3 months (Figure 1b), we observed two mixed phases: a c(4 × 2) superlattice

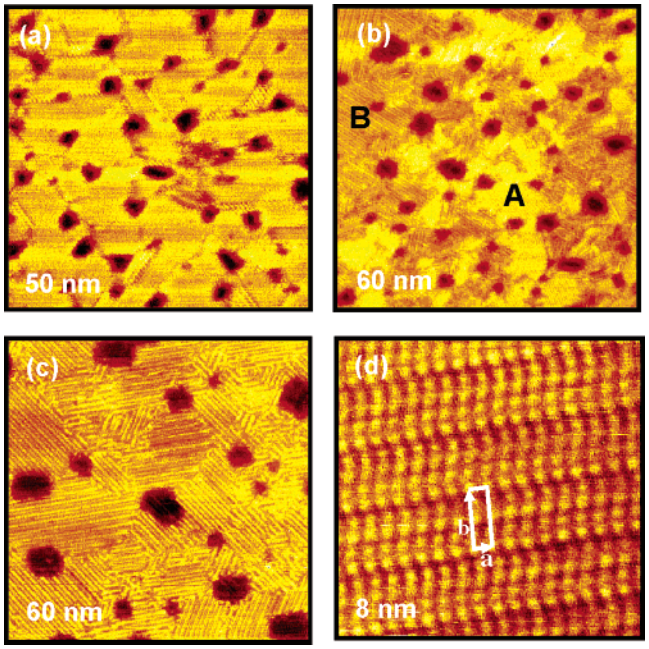

Figure 1. STM images showing the phase transitions of OT SAMs on Au(111) from the c(4 × 2) phase to the new (6 × √3) phase depending on the long-term storage at room temperature: (a) the c(4 × 2) superlattice obtained from a SAM sample after 1 day of deposition (50 nm × 50 nm, $V_b = 0.43$ V, and $I_t = 0.25$ nA); (b) two mixed phases consisting of the c(4 × 2) superlattice and the (6 × √3) phase appeared after 3 months (60 nm × 60 nm, $V_b = 0.83$ V, and $I_t = 0.12$ nA); (c) the (6 × √3) phase appeared after 6 months (60 nm × 60 nm, $V_b = 0.60$ V, and $I_t = 0.19$ nA); (d) high-resolution STM image of the (6 × √3) phase (8 nm × 8 nm, $V_b = 0.60$ V, and $I_t = 0.19$ nA). The lattice constants of the rectangular unit cell are $a = \sqrt{3}a_h = 4.9$ Å and $b = 6a_h = 17.5$ Å, where $a_h = 2.89$ Å denotes the interatomic spacing of the Au(111) lattice.

(A phase) and a new phase containing linear molecular rows (B phase). After 6 months (Figure 1c), the c(4 × 2) superlattice completely disappeared and a single domain structure with linear molecular rows (B phase) was formed. The high-resolution STM image for B phase in Figure 1d shows a rectangular unit cell with cell dimensions of 4.9 Å × 17.5 Å containing four alkanethiols, which can be described as a (6 × √3) superlattice. It was confirmed that the surface coverages of these two structures were nearly identical, indicating that such time-dependent structural transitions were not due to a change of surface coverage. Further structural details were described in our recent communication paper.[32]

As mentioned in the Introduction, one of the purposes of this study was to examine time-dependent interfacial dynamics of sulfur headgroups, such as a conversion of adsorption sites and/or dimerization of sulfur headgroups in the process of two-dimensional structural transitions dependent on time evolution. Figure 2 shows the time evolution of the HREEL spectra for OT SAMs on Au(111). Corresponding to the STM results, the interface features of OT SAMs depending on long-term storage were observed (a) from as-deposited SAMs (Figure 2a), (b) after 3 months of storage of as-deposited SAMs (Figure 2b), and (c) after 6 months of storage of as-deposited SAMs (Figure 2c). All samples were kept under a vacuum at approximately 400 Torr at room temperature, until introduction into the HREELS sample entry chamber. In Figure 2, the sets of specular and off-specular spectra are plotted to clarify the dipole- and impact-scattering components. In the specular spectrum, the dipole-scattering components are the additive components of the impact-scattering ones estimated from its off-specular spectrum.

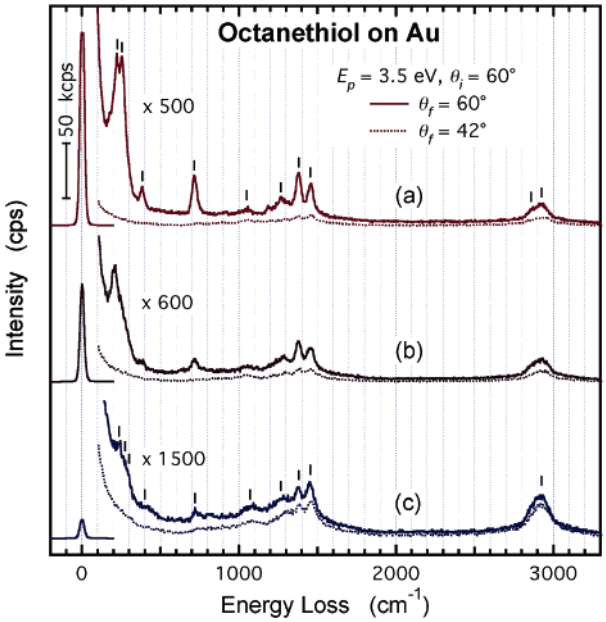

Figure 2. HREEL spectra for OT SAMs on Au(111) depending on the long-term storage at room temperature: (a) as-deposited SAMs; (b) after 3 months of storage of as-deposited SAMs; (c) after 6 months of storage of as-deposited SAMs. The specular spectrum (solid line) and the off-specular spectrum (dotted line) were measured at detection angles of 60 and 42°, respectively, with respect to the surface normal. The off-specular spectra were plotted with an intensity factor of cos 60°/cos 42° in order to expect the impact-scattering components in the specular spectra.

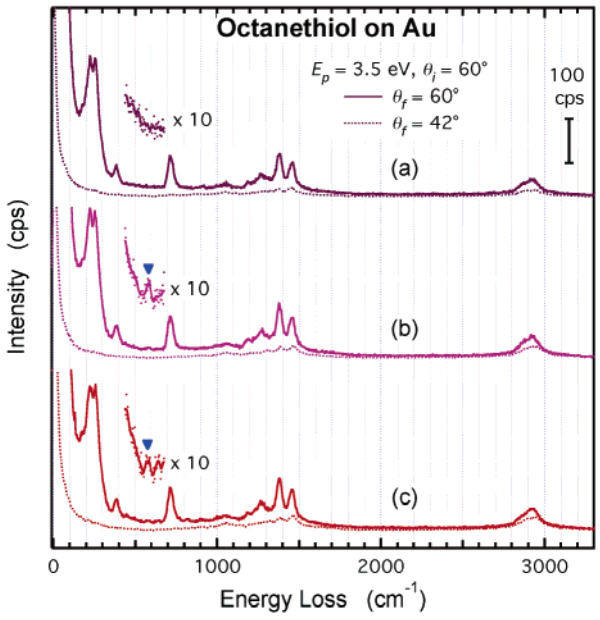

Figure 3. HREEL spectra for the annealed OT SAMs on Au(111): (a) before annealing; (b) after annealing at 50 °C for 30 min in a N_2 atmosphere of 1 atm; (c) after annealing at 100 °C for 30 min in a N_2 atmosphere of 1 atm. The specular spectrum (solid line) and the off-specular spectrum (dotted line) were measured at detection angles of 60 and 42°, respectively, with respect to the surface normal. The off-specular spectra were plotted with an intensity factor of cos 60°/cos 42° in order to expect the impact-scattering components in the specular spectra.

TABLE 1: Vibrations of Octanethiol SAMs on Au(111) Observed by HREELS[a]

vibrational mode	as-deposited SAMs	after 6 months
C−H stretch	2925	2925
	2860	
CH_3 d-deform	1455	1455
CH_2 scissors	1455	1455
CH_3 s-deform	1380	1380
CH_2 twist	1265	1265
C−C stretch	1050	1070
CH_2 rock	715	720
SCC deform	385	≈400
CCC deform	385	≈400
Au−S stretch	255	≈300
	225	275
		235

[a] Vibration frequencies are given in wavenumbers (cm^{-1}). The accuracy is about ±10 cm^{-1}.

The vibration modes of the c(4 × 2)-phase alkanethiol SAMs on Au have been extensively examined and precisely assigned in previous studies,[9,12,13,29,37−41] as listed in Table 1. Briefly, they include the C−H stretching modes at 2800−3000 cm^{-1}, the C−H bending modes at 700−1500 cm^{-1}, and the Au−S stretching modes at 200−300 cm^{-1}. Large dipole-scattering signals were obtained from the as-deposited SAM samples containing a c(4 × 2) superlattice, as shown in Figure 1a. Over time, the intensity of the dipole-scattering components decreased, showing a decrease in elastic-peak intensity, while the impact-scattering components did not change significantly. The intensity decrease in the dipole-scattering components could be due to an order−disorder phase transition or a structural change in an ordered layer. The intensity enhancement in the HREELS measurements at the specular position occurs from electron diffraction on the surfaces. As with structural analysis in low-energy electron diffraction (LEED), the intensity of electron diffraction is influenced not only by the two-dimensional superstructures but also by the local configurations of the surface atoms. Since the ordered (6 × √3) superstucture was observed from the 6-month OT SAM sample, as shown in Figure 1c, the intensity decrease of the dipole-scattering components in Figure 2 must be caused by a structural change in the ordered layer.

In the HREEL spectra for time evolution, the observed vibration modes of alkyl chains do not show significant frequency shifts, as indicated in Figure 2c and listed in Table 1, but their relative intensities do change. In addition, when we annealed the OT SAM samples at 100 °C for 30 min at 1 atm, an additive loss peak at 1720 cm^{-1} was observed (not shown here). The additive loss peak is assigned to a C═O stretching mode[42] formed by the oxidation of SAMs during annealing. Therefore, we are confident that the structural transitions from the c(4 × 2) superlattice to the (6 × √3) superlattice are not caused by chemical reactions but caused by the structural transitions of OT SAMs, as observed in the STM measurements.

The most interesting feature in the time evolution is the change in the Au−S stretching modes. Two intense peaks of Au−S stretching modes were observed at 225 and 255 cm^{-1} from the as-deposited OT SAM samples (Figure 2a). With time evolution (after 3 and 6 months), the Au−S stretching modes broadened, as shown in Figure 2b and c. In the energy resolution under our experimental conditions, the broad peak should consist of at least three components (235, ≈275, and ≈300 cm^{-1}), as indicated in Figure 2c. Note that the highest energy component is the minority in the HREEL spectrum of the as-deposited SAM sample. According to the nearest-neighbor force-constant model,[43] the variety of the Au−S stretching frequencies is attributed to the existence of several available adsorption sites. Consequently, three types of adsorption sites for sulfur headgroups adsorbed on Au(111) (hollow, bridge, and atop sites) are available for OT SAMs after the structural phase transitions in this time evolution. Therefore, it can be considered that the dynamic movement of adsorption sites for sulfur headgroups, from two

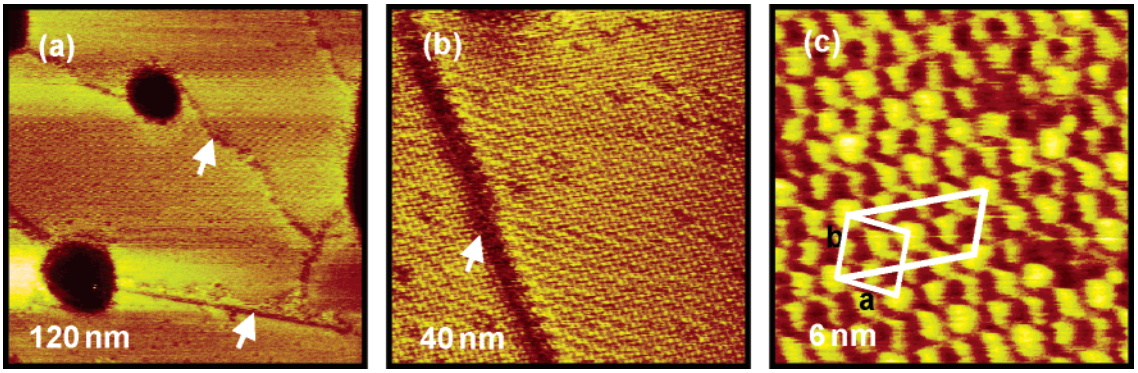

Figure 4. STM images showing surface structures of the annealed OT SAMs at 100 °C for 30 min: (a) the sizes of ordered c(4 × 2) domains and vacancy islands were enlarged (120 nm × 120 nm, $V_b = 0.40$ V, and $I_t = 0.35$ nA); (b and c) molecularly resolved c(4 × 2) structures ((b) 40 nm × 40 nm, $V_b = 0.50$ V, and $I_t = 0.25$ nA; (c) 6 nm × 6 nm, $V_b = 0.50$ V, and $I_t = 0.25$ nA). Note that a $(3 \times 2\sqrt{3})$ structure is commonly called a c(4 × 2) superlattice: the lattice constants of the unit cell were measured to be $a = 8.5 \pm 0.2$ Å and $b = 9.8 \pm 0.2$ Å, which can be assigned as a $(3 \times 2\sqrt{3})$ structure.

to three adsorption sites, is the main driving force for the phase transition from the c(4 × 2) superlattice to the $(6 \times \sqrt{3})$ superlattice. The conversion of adsorption sites in SAMs would give rise to changes in the orientation of alkyl chains by the twisting of the alkyl chains about the chain axis. As a result, the new $(6 \times \sqrt{3})$ superlattice can be formed, as shown in Figure 1. In addition, we clearly demonstrated that this phase transition is not related to the dimerization of sulfur headgroups because the time-evolved SAM samples did not contain the S−S stretching modes previously assigned.[13] From this result, it is concluded that the chemical structure of the sulfur headgroups does not change, even after long-term storage at room temperature.

In contrast to the drastic changes of the HREELS spectra in the long-term-stored SAM samples, as described above, the HREEL spectra for the annealed OT SAMs on Au(111) show only very few changes, as shown in Figure 3. The samples in this experiment were annealed at 50 °C for 30 min (Figure 3b) or at 100 °C for 30 min (Figure 3c) in a N_2 atmosphere of 1 atm. All of the HREEL spectra of the annealed samples (Figure 3b and c) are nearly identical with that of the as-deposited sample (Figure 3a). In particular, the two intense peaks of the Au−S stretching modes do not change at all after annealing. This implies that these short-time annealing procedures do not affect the adsorption sites of sulfur atoms. Contrary to the HREELS results, after annealing OT SAMs at 100 °C for 30 min in a N_2 atmosphere, the surface characteristics of the OT SAMs were markedly changed (Figure 4a). For instance, the sizes of the ordered domains and vacancy islands (VIs) were enlarged and the number of VIs decreased steeply, as shown in previous papers.[2−4] However, despite the many structural changes after annealing, the c(4 × 2) domain phases from the annealed SAM samples were observed as a main domain structure, shown in Figure 4b and c, as with the as-deposited OT SAM samples (Figure 1a),[19,22] This result indicates that the structural transition of the closely packed c(4 × 2) domain would not occur from the annealing processes.[44−46] Even though a large variation of surface structures resulting from a facile dynamic movement of gold atoms by thermal annealing arises, the fact that the adsorption sites are not changed in the crystallized, ordered c(4 × 2) domains is surprising. This result suggests that the crystallized c(4 × 2) phase is very stable and the modification of the adsorption sites for sulfur atoms is not favorable. However, we found that the conversion of adsorption sites for sulfur atoms will only occur by temporal function. Very slow rearrangement processes of SAMs accompanied by the conversion of adsorption sites are responsible for the phase transition from the c(4 × 2) superlattice to the $(6 \times \sqrt{3})$ superlattice, and the resulting energy gain may be overwhelming the energy gain derived from the formation of the c(4 × 2) phases.

In addition, a small loss peak from the annealed SAM samples was only detected at 575 cm^{-1}, which can be assigned to the S−S stretching modes, as previously observed after the annealing procedure.[13] It has been known that dialkyl disulfide is thermally desorbed from alkanethiol SAMs on Au(111).[28] Thus, the appearance of the small S−S stretching peak could be attributed to the existence of a small amount of dimerized species in a metastable precursor state for desorption. The small amount of dimers should be more easily formed around VIs, step edges, and/or structural defects, as indicated by the arrows in Figure 4, because the dimerization processes resulting from the associative reaction of sulfur atoms occur much more easily at loosely packed regions. Note that the c(4 × 2) superlattice is not related to the dimerization of sulfur headgroups, as suggested by Fenter et al.[27] It is generally believed that alkanethiol SAMs prepared at room temperature consist of alkanethiolate monomers,[12] and the various alkanethiolate monomers have a stable c(4 × 2) structure.[2,19−22] In this study, if the c(4 × 2) superlattice observed as a main domain structure is related to the dimer, the intensity of the HREEL spectrum for the S−S stretching modes is expected to be very strong, but here, it was found to be very weak. This result strongly implies that the c(4 × 2) superlattice of alkanethiol SAMs on Au(111) is not related to the dimerization of sulfur headgroups.

Conclusion

From our STM and HREELS measurements, we have demonstrated that the structural transitions of OT SAMs from the c(4 × 2) superlattice to the $(6 \times \sqrt{3})$ superlattice depending on long-term storage occur from the dynamic movement of adsorption sites for sulfur headgroups from two to three sites. The conversion of adsorption sites in SAMs can give rise to changes in orientation of the alkyl chains. As a result, the new $(6 \times \sqrt{3})$ superlattice can be formed, as revealed by STM. In addition, this phase transition is not related to the dimerization of sulfur headgroups, as we observed no S−S stretching modes for the time-evolved SAM samples, which indicates that the Au−S chemical bonds are highly stable in SAMs. In contrast to the drastic changes in the HREELS spectra for the long-term-stored SAM samples, the HREEL spectra for the annealed OT SAMs on Au(111) show very few changes. In particular, it was observed that two intense peaks of Au−S stretching modes do not change at all after annealing, implying that these short-

time annealing procedures do not affect the adsorption sites of sulfur atoms. Moreover, it is considered that the c(4×2) superlattice is not directly related to the dimerization of sulfur headgroups. We are confident that our results will provide a basis for gaining a better understanding of the interface dynamics and stability of sulfur atoms in SAMs on an Au(111) surface.

Acknowledgment. Financial support for the present study was provided in part by the Grant-in-Aid for Scientific Research on Priority Areas "Surface Chemistry of Condensed Molecules" from the Ministry of Education, Culture, Sports, Science and Technology of Japan.

Note Added after ASAP Publication. CCC deform values and Au−S stretch values in Table 1 have been corrected. This paper was published on the Web on 1/7/06. The corrected version was posted on 1/20/06.

References and Notes

(1) Ulman, A. *Chem. Rev.* **1996**, *96*, 1533.
(2) Poirier, G. E. *Chem. Rev.* **1997**, *97*, 1117.
(3) Love, J. C.; Estroff, L. A.; Kriebel, J. K.; Nuzzo, R. G.; Whitesides, G. M. *Chem. Rev.* **2005**, *105*, 1103.
(4) Yang. G.; Liu, G.-y. *J. Phys. Chem. B* **2003**, *107*, 8746.
(5) Schreiber, F. *Prog. Surf. Sci.* **2000**, *65*, 151.
(6) Schreiber, F. *J. Phys.: Condens. Matter* **2004**, *16*, R881.
(7) Cheng, L.; Yang, J.; Yao, Y.; Price, D. W.; Dirk, S. M.; Tour, J. M. *Langmuir* **2004**, *20*, 1335.
(8) Motesharei, K.; Myles, D. C. *J. Am. Chem. Soc.* **1998**, *120*, 7328.
(9) Nuzzo, R. G.; Dubois, L. H.; Allara, D. L. *J. Am. Chem. Soc.* **1990**, *112*, 558.
(10) Poirier, G. E.; Pylant, E. D. *Science* **1996**, *272*, 1145.
(11) Poirier, G. E. *Langmuir* **1999**, *15*, 1167.
(12) Kato, H. S.; Noh, J.; Hara, M.; Kawai, M. *J. Phys. Chem. B* **2002**, *106*, 9655.
(13) Kluth, G. J.; Carraro, C.; Maboudian, R. *Phys. Rev. B* **1999**, *59*, R10449.
(14) Ishida, T.; Hara, M.; Kojima, M.; Tsuneda, S.; Nishida, N.; Sasabe, H.; Knoll, W. *Langmuir* **1998**, *14*, 2092.
(15) Nuzzo, R. G.; Fusco, F. A.; Allara, D. L. *J. Am. Chem. Soc.* **1987**, *109*, 2358.
(16) Strong, L.; Whitesides, G. M. *Langmuir* **1988**, *4*, 546.
(17) Chidsey, C. E. D.; Liu, G.-Y.; Scoles, G.; Wang, J. *Langmuir* **1990**, *6*, 1804.
(18) Sellers, H.; Ulman, A.; Shnidman, Y.; Eilers, J. E. *J. Am. Chem. Soc.* **1993**, *115*, 9389.
(19) Poirier, G.; Tarlov, M. J. *Langmuir* **1994**, *10*, 2853.
(20) Delamarche, E.; Michel, B.; Gerber, C.; Anselmetti, D.; Güntherodt, H.-J.; Wolf, H.; Ringsdorf, H. *Langmuir* **1994**, *10*, 2869.
(21) Noh, J.; Hara, M. *Langmuir* **2001**, *17*, 7280.
(22) Kobayashi, K.; Yamada, H.; Horiuchi, T.; Matsushige, K. *Jpn. J. Appl. Phys.* **1998**, *37*, 6183.
(23) Müller-Meskamp, L.; Lüssem, B.; Karthäuser, S.; Waser, R. *J. Phys. Chem. B* **2005**, *109*, 11424.
(24) Lüssem, B.; Müller-Meskamp, L.; Karthäuser, S.; Waser, R. *Langmuir* **2005**, *21*, 5256.
(25) Fenter, P.; Eberhardt, A.; Eisenberger, P. *Science* **1994**, *266*, 1216.
(26) Yeganeh, M. S.; Dougal, S. M.; Polizzotti, R. S.; Rabinowitz, P. *Phys. Rev. Lett.* **1995**, *74*, 1811.
(27) Fenter, P.; Schreiber, F.; Berman, L.; Scoles, G.; Eisenberger, P.; Bedzyk, M. *Surf. Sci.* **1998**, *412/413*, 213.
(28) Nishida, N.; Hara, M.; Sasabe, H.; Knoll, W. *Jpn. J. Appl. Phys.* **1996**, *35*, L799.
(29) Hayashi, T.; Morikawa, Y.; Nozoye, H. *J. Chem. Phys.* **2001**, *114*, 7615.
(30) Morikawa, Y.; Hayashi, T. *Surf. Sci.* **2002**, *507−510*, 46.
(31) Vargas, M. C.; Giannozzi, P.; Selloni A.; Scoles, G. *J. Phys. Chem. B* **2001**, *105*, 9509.
(32) Noh, J.; Hara, M. *Langmuir* **2002**, *18*, 1953.
(33) Noh, J.; Murase, T.; Nakajima, K.; Lee, H.; Hara, M. *J. Phys. Chem. B* **2000**, *104*, 7411.
(34) Kato, H.; Okuyama, H.; Ichihara, S.; Kawai, M.; Yoshinobu, J. *J. Chem. Phys.* **2000**, *112*, 1925.
(35) Ibach, H.; Mills, D. L. *Electron energy loss spectroscopy and surface vibrations*; Academic Press: New York, 1982; Chapter 3.
(36) Ibach, H. *Surf. Sci.* **1977**, *66*, 56.
(37) Nuzzo, R. G.; Zegarski, B. R.; Dubois, L. H. *J. Am. Chem. Soc.* **1987**, *109*, 733.
(38) Porter, M. D.; Bright, T. B.; Allara, D. L.; Chidsey, C. E. D. *J. Am. Chem. Soc.* **1987**, *109*, 3559.
(39) Bryant, M. A.; Pemberton, J. E. *J. Am. Chem. Soc.* **1991**, *113*, qj8284.
(40) Chang, S.-C.; Chao, I.; Tao, Y.-T. *J. Am. Chem. Soc.* **1994**, *116*, 6792.
(41) Hayashi, T.; Fricke, A.; Katsura, K.; Kodama, C.; Nozoye, H. *Surf. Sci.* **1999**, *427−428*, 393.
(42) Shimanouchi, T. *NSRDS-NBS 39, Tables of Molecular Vibrational Frequencies, Consolidated Volume I*; U.S. Department of Commerce, 1972.
(43) Ibach, H.; Mills, D. L. *Electron energy loss spectroscopy and surface vibrations*; Academic Press: New York, 1982; Chapters 4.2.2 and 6.2.1.
(44) Xiao, X.; Wang, B.; Zhang, C.; Yang, Z.; Loy, M. M. T. *Surf. Sci.* **2001**, *472*, 41.
(45) Camillone, N., III; Eisenberger, P.; Leung, T. Y. B.; Schwartz, P.; Scoles, G. Poirier, G. E.; Tarlov, M. J. *J. Chem. Phys.* **1994**, *101*, 11031.
(46) Fukuma, T.; Ichii, T.; Kobayashi, K.; Yamada, H.; Matsushige, K. *J. Appl. Phys.* **2004**, *95*, 1222.